NAVAL RESEARCH REVIEWS

APRIL 1971

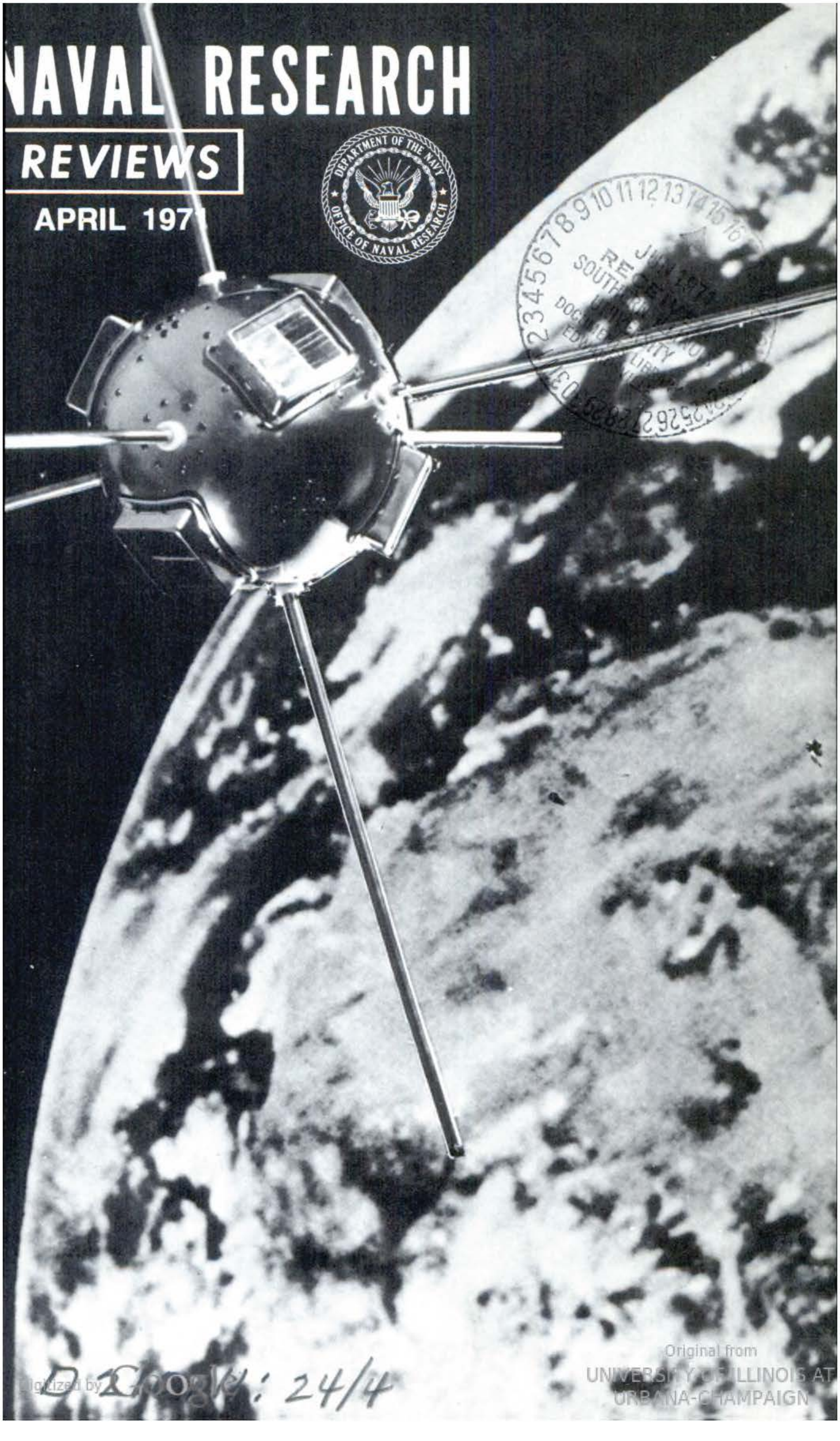

PROFILES IN SCIENCE

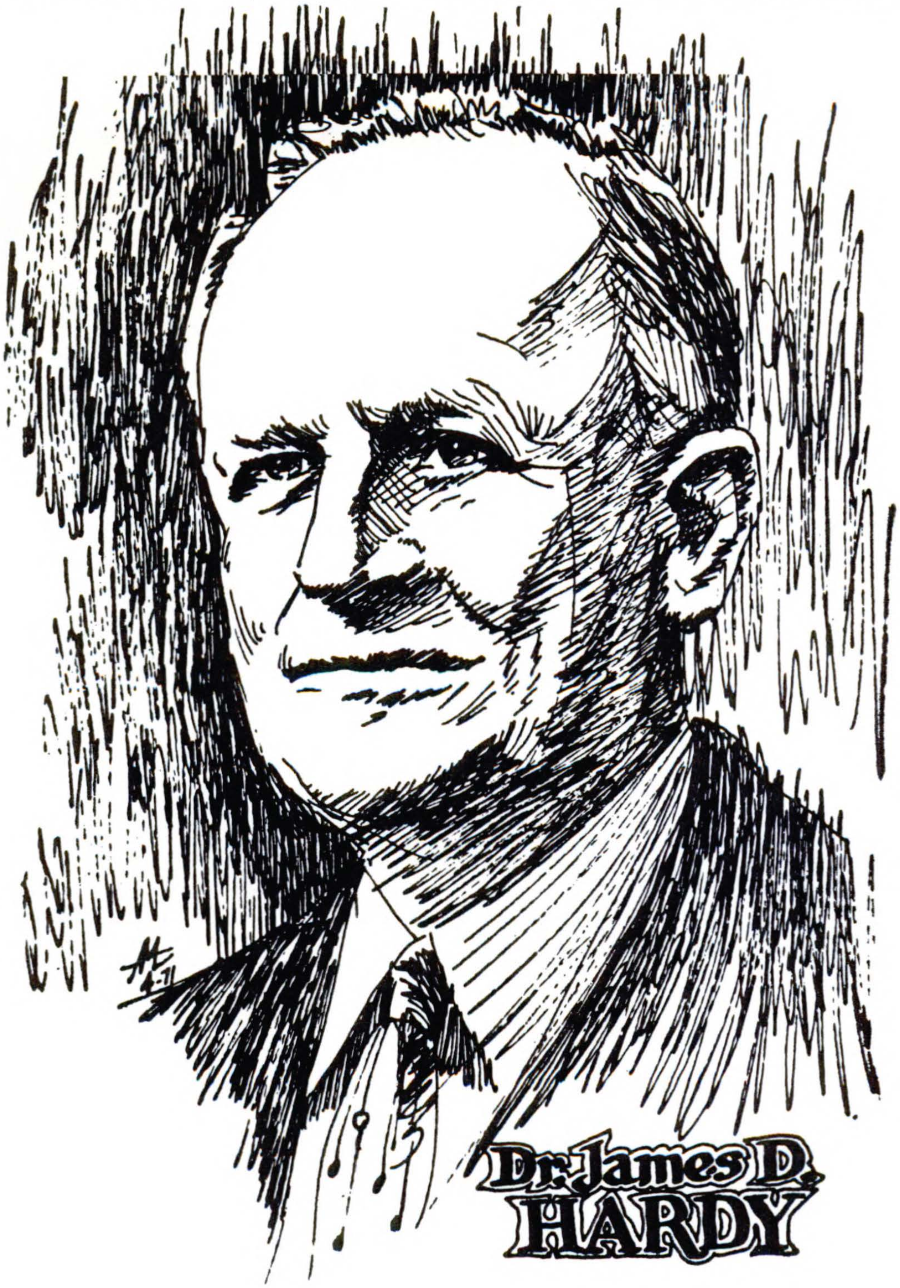

Dr. James D. Hardy, an authority in the physiological mechanisms of body temperature control, early in his career completed a series of classic studies on human calorimetry and succeeded in quantifying heat exchange phenomena in man.

After World War II Dr. Hardy conducted aerospace medical research. From 1953 to 1961 he was Chief Scientist at the Aviation Medical Acceleration Laboratory and a professor at the University of Pennsylvania. Since 1961 Dr. Hardy has been Director of the John B. Pierce Foundation in New Haven and simultaneously a professor at Yale Medical School.

Dr. Hardy's association with the Navy began during World War II commanding a mine sweeper. He continued in the Naval Reserve from which he retired in 1964 as a Rear Admiral. Since its early days, Dr. Hardy has been a leading contractor for ONR.

The Search for Fusion Power

CDR G. J. Mischke*
Office of Naval Research

Some 40 years ago, astrophysicists showed that the energy of our sun and of similar stars results from fusion reactions. This same type of energy, harnessed as heavy hydrogen fusion on earth, could produce a virtually unlimited source of energy for man—a source with many potential advantages over all other sources of energy. Fusion reactions were first produced on earth in the 1920's by using high energy particle accelerators to accelerate protons (hydrogen nuclei) through the nuclear electrical repulsion and force the protons to fuse with light nuclei in a target. Also, uncontrolled fusion was accomplished in the hydrogen bomb in the early 1950's. Fusion reactions release energy because part of the mass of the fusing nuclei is transformed into energy according to Einstein's energy-mass relationship. However, fusion using accelerator bombardment requires a great deal more energy to fuse the nuclei than is obtained in return, and fusion from the hydrogen bomb principle results in an uncontrolled release of energy. To obtain useful energy from fusion reactions requires the reactions to proceed in a self-sustaining manner, whether continuously or in pulses.

In order to see how controlled fusion may be realized, consider the nature of the fusion process. Fusion reactions are rearrangement reactions which occur between low atomic number (Z) nuclei such as hydrogen (H), deuterium (H^2 or D), tritium (H^3 or T), and helium 3 (He^3). For fusion to occur, the two light nuclei must collide or pass close enough to permit interaction to take place. This requires the nuclei to have enough energy to overcome the force of electrostatic repulsion of their nuclear positive electrical charge. The magnitude of the repelling force is proportional to the product of the charges on the two nuclei, making the low Z nuclei the primary contenders for fusion reactions. Some useful nuclear reactions for the production of fusion power are listed in Table I. In these reactions, the resulting nuclei are less massive than the original pair, and as predicted by Einstein's equation $E = mc^2$, this difference in mass is released as kinetic energy of the resulting nuclei. Following each reactant in Table I (in parentheses) is the amount of energy the resulting nuclei acquires in millions of electron volts (Mev) where 1 Mev $= 3.83 \times 10^{-4}$ calories. Reactions (1) and (2) occur with

CDR Mischke is the Energy Conversion Project Officer for the Office of Naval Research. He enlisted in the Navy in 1949 and was commissioned in 1952 after completing flight training. CDR Mischke then served with Fighter Squadron 32 and later attended the University of Minnesota. In 1960 he was assigned to the Nuclear Engineering course at the Naval Postgraduate School where he received a MS in physics. His recent duties include Operations Officer Attack Squadron 155, Research Associate at the Lawrence Radiation Laboratory, and Nuclear Weapons Development Officer at Headquarters, Defense Atomic Support Agency.

TABLE I

Fusion Reactions

(1) $D + D \longrightarrow He^3(0.8) + n(2.45)$

(2) $D + D \longrightarrow T\ (1.0) + H(3.0)$

(3) $D + T \longrightarrow He^4(3.5) + n(14.1)$

(4) $D + He^3 \longrightarrow He^4(3.6) + H(14.7)$

roughly equal probability. Reactions (3) and (4) are of particular interest in view of their high energy yield plus they involve the reaction products of (1) and (2). The energy required to promote these fusion reactions is roughly one percent of the energy released in the fusion reaction itself giving the available energy payoff ratio. As shown by the reactions in Table I, the essential fuel material is deuterium D (heavy hydrogen) which is present in water. For every 6500 or so atoms of ordinary hydrogen in water, there is one atom of deuterium. In theory, the energy that could be produced by the fusion of the deuterium nuclei present in a gallon of water is about equal to that obtainable from the combustion of 300 gallons of gasoline. With the cost of deuterium extraction per gallon of water being less than ten cents and the vast amounts of water available on earth, this appears to be the ideal energy source. However, this is not the whole story. For one thing, as in a nuclear fission reactor, the price of the fuel represents only a small portion of the cost of the electrical power produced. Also, there are tremendously difficult scientific problems to be solved before fusion power can be a reality.

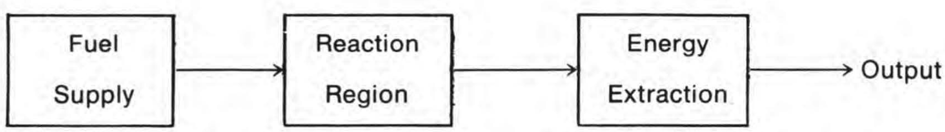

Figure 1 — Block diagram of an energy conversion system (see Ref. 2)

A simplified diagram of an energy conversion system is shown in Figure 1. At this point, the fuel supply can be provided by deuterium and the required fusion reactions are shown in Table I. The requirements for an economical fusion reactor on earth are to create a plasma at an ultrahigh temperature, contain the plasma long enough for the nuclei to react and extract the resultant energy in a useful form. In the sun and stars, nuclear fusion reactions occur as a result of the high temperature in the stellar core. Containment is provided by the associated gravitational field and the energy is radiated as heat and light. To produce fusion on earth, we must heat the fusion fuel to a kindling temperature above 20 million degrees K. At such temperatures, the fuel is a plasma, a fully ionized gas composed of free electrons and positively charged ions with thermal velocities of several thousand miles per second. One of the main difficulties lies in the insulation of the high temperature plasma from the walls of its container. Since the plasma has an enormous thermal conductivity, insulation is essential or the energy would escape to the container walls and the required high temperature could not be attained. As will be seen later, the plasma must be contained in a relatively high vacuum and the primary containment mechanism is a magnetic field. Other forms of containment may be possible, however, they do not appear to be as promising as magnetic containment.

When the plasma is heated and confined, the resulting fusion energy must be extracted and converted into a useful form. As shown by the reactions in Table I, the fusion energy remains with the reactant products—neutrons and charged nuclei. The neutron energy can be recovered by slowing the neutrons in a surrounding blanket, called a moderating blanket. This neutron energy, changed to heat in the moderating blanket, can be utilized by conventional boilers and turbines. Theoretical and experimental studies indicate that the plasma charged particle energy can be converted directly to electricity with high efficiencies. Direct conversion of plasma energy to electricity could give preference to the D-He^3 reaction—reactant energy high and reactant products charged. However, the reactor fuel proportions (D, T, He^3) are dependent on fundamental research to determine fusion feasibility and to determine the most practical fusion energy conversion technique.

The general requirements for an ultrahigh temperature plasma to be contained by a magnetic field have been outlined. Now, what are the physical parameters such as temperature, density and containment field strength required to utilize a fusion plasma as an energy source for a power reactor?

Fusion Parameters and Plasma Containment

There are a number of physical conditions which must be met for fusion reactions to take place. One of the physical parameters is the fusion reaction cross section σ. This cross section is proportional to the probability that a fusion reaction will occur between a given pair of nuclei. Figure 2 shows the measured values of cross section in barns (1 barn = 10^{-24} cm^2) as a function of the deuteron energy for the fusion reactions given in Table I. The deuteron energy is given in units of kiloelectron volts (kev) where 1 kev kinetic energy is approximately 1.6×10^{-16} joules or watt sec. Fusion energy is released since the mass of the reactant products is less than the mass of the original nuclei. This mass change energy can be related to the interplay of the cohesive nuclear constituents of the nucleus (protons and neutrons). These

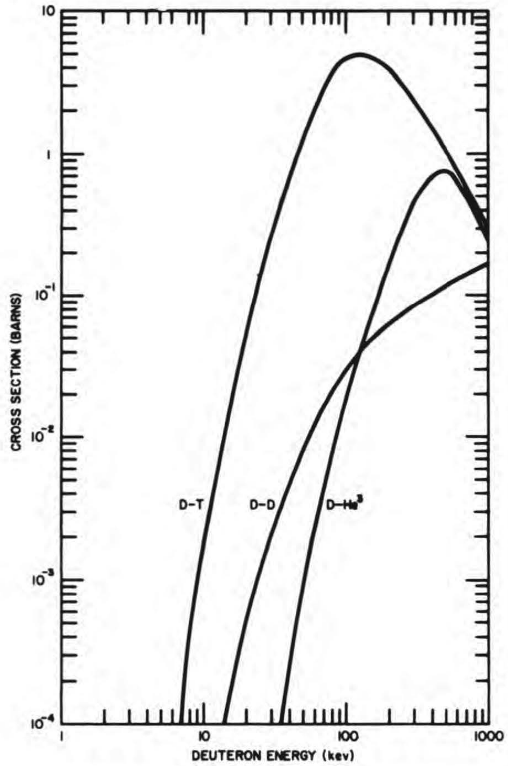

Figure 2 – Cross section for D-T, D-D (total), and D-He^3 reactions (see Ref. 1)

nuclear forces are effective over a small distance—of the order of the nucleus diameter or about 10^{-13} centimeters. Superimposed on the nuclear forces are electrostatic repulsive coulomb forces due to the positively charged protons in the nucleus. Overcoming this coulomb repulsion is accomplished by increasing the energy or relative velocity (v) of the reacting nuclei to promote the probability of mutual collisions. Suppose a group of fusion ions with a kinetic temperature T are mutually colliding. The probability per unit time that a given ion n_T will react with another ion n_D will be given by the product of the reaction cross section σ, the relative velocity v_{DT} and the particle densities of n_T and n_D. The reaction rate per unit volume is

$$R_{DT} = n_T n_D \overline{\sigma v_{DT}} \text{ reactions/cm}^3\text{sec.} \qquad (1)$$

The averaged product $\overline{\sigma v_{DT}}$ can be determined as a function of energy or temperature by assuming Maxwellian velocity distribution for the particles in conjunction with the known reaction cross sections from Figure 2.

With the information developed for Equation (1) and the reaction energies from Table I, representative power densities can be calculated as a function of the particle density for the fusion fuels. The fusion power P released in a cubic centimeter of reacting plasma may be written as

$$P = n_T n_D \overline{\sigma v_{DT}} \, Q_{DT} \text{ watts/cm}^3. \qquad (2)$$

This is the reaction rate (Equation (1)) times Q_{DT}, the energy of the reactant charged particles for the *D-T* reaction. Only the energy of the charged particles will be retained within the reaction region. The neutrons will escape from the reaction region and deposit their energy elsewhere. Therefore, only the reactant charged particle energies will be available internally to compensate for energy losses and to sustain fusion reactions. With this restriction on Q, the power density values using Equation (2) are shown in Figure 3 as a function of the reacting particle density. An operating temperature of 100 kev was selected as representative where 1 kev kinetic temperature equals 1.16×10^{7}°K. It will be shown later that operation at a kinetic temperature an order of magnitude lower is at best marginal. The curves for D-D, D-T, and D-He^3 in Figure 3 are compared with 100 watts/cm^3 which is of the same order power density as found in fission reactors. A power density of 10 watts/cm^3 for a continuously operating (steady-state) or 1000 watts/cm^3 for a pulsing fusion reactor system may be practical. The operating power density will be determined by the material and the engineering constraints for the power plant. Using 100 watts/cm^3 as a representative fusion reactor power density, the resulting fuel particle density is between 10^{15} and 10^{16} particles/cm^3 as shown in Figure 3. These particle

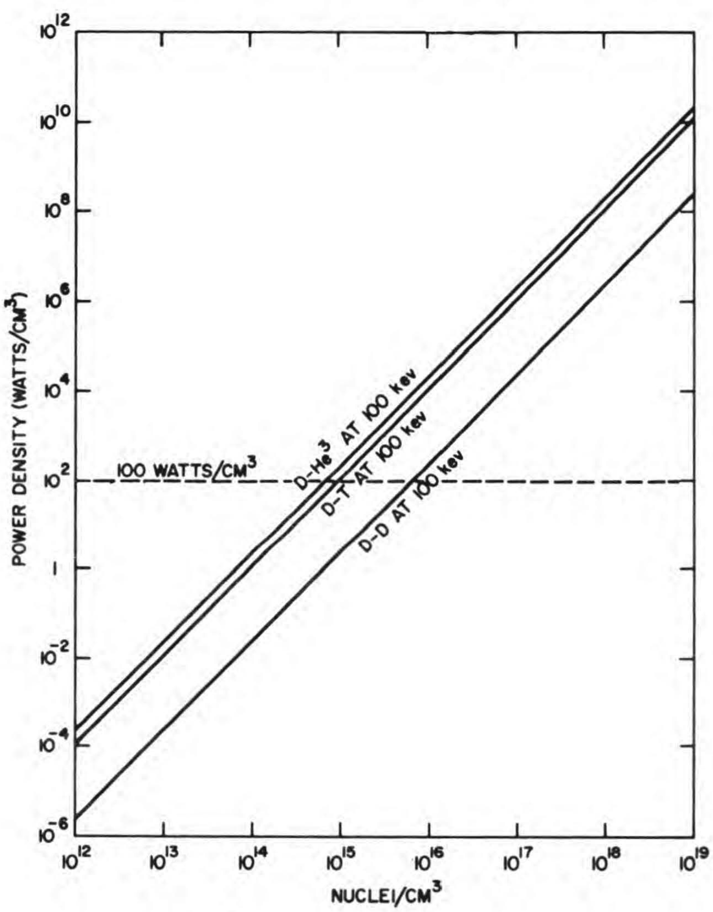

Figure 3 — Power densities for D-T, D-D (total) and D-He^3 reactions at $T = 100$ kev.

densities correspond to about 10^{-5} to 10^{-4} times atmospheric density at sea level.

The discussion so far refers to power which may be produced in a fusion reactor. This power production must compete with inevitable losses. The minimum temperature for operation of a fusion reactor is set by the balance between fusion energy production and radiation losses. At the kinetic temperatures of interest, the plasma in a fusion reactor will consist of completely stripped nuclei of hydrogen isotopes and helium 3 with the corresponding number of electrons. From such a plasma, energy will inevitably be lost in the form of bremsstrahlung, that is, continuous radiation emitted by charged particles (mainly electrons) as a result of deflection by the coulomb fields of other charged particles. For plasma kinetic temperatures up to about 100 kev, bremsstrahlung is the predominant form of radiation which results mainly from electron-ion interactions. Assuming the electron temperature equals the ion temperature, the bremsstrahlung power radiated P_{br} can be expressed as

$$P_{br} = 5.35 \times 10^{-31} T_e^{1/2} n_e \Sigma (n_i Z^2) \text{ watts/cm}^3 \tag{3}$$

where the temperature T is expressed in kev, n_e the number density of electrons, n_i the number density of ions and Z is the nuclei atomic number. For a plasma consisting only of deuterium, Z is 1 and n_i equals n_e, so the factor $n_e \Sigma (n_i Z^2)$ may be replaced by n_D^2. For a 50 atomic percent mixture of deuterium and tritium or deuterium and helium 3, the $n_e \Sigma (n_i Z^2)$ factor may be replaced by $4 n_D n_T$ and $15 n_D n_{He^3}$, respectively. Equations (2) and (3) are shown in Figure 4 as a function of the kinetic temperature of the plasma. The information in Figure 4 assumes n_D as 10^{15} nuclei/cm³ for the D-D reactions, where n_D, n_T, and n_{He^3} are each 0.5×10^{15} nuclei for the D-T and D-He³ reactions. Where the local fusion energy equals the bremsstrahlung radiation, it is shown that the minimum plasma ignition temperature is about 4 kev for D-T, 36 kev for D-D and 34 kev for D-He³ reactions. The minimum plasma ignition temperature is an idealized condition since in real cases additional losses, such as thermal conduction and cyclotron radiation, will require an increased operating temperature. Also, the calculated bremsstrahlung radiation assumed no high Z impurities in the plasma. Suppose, for example, the impurity is oxygen ($Z = 8$) and it consists of one atomic percent of the plasma. Using Equation (3), the oxygen impurity will increase the rate of bremsstrahlung energy loss by about 77 percent. Using Figure 4, this increase in bremsstrahlung would increase the ideal ignition temperature from 36 to 80 kev for the D-D system, from 34 to 45 kev for the D-He³ system, and from 4 to 5.5 kev for the D-T system. This brings out another important requirement for a fusion plasma; that is, traces of impurities, especially those of moderate and

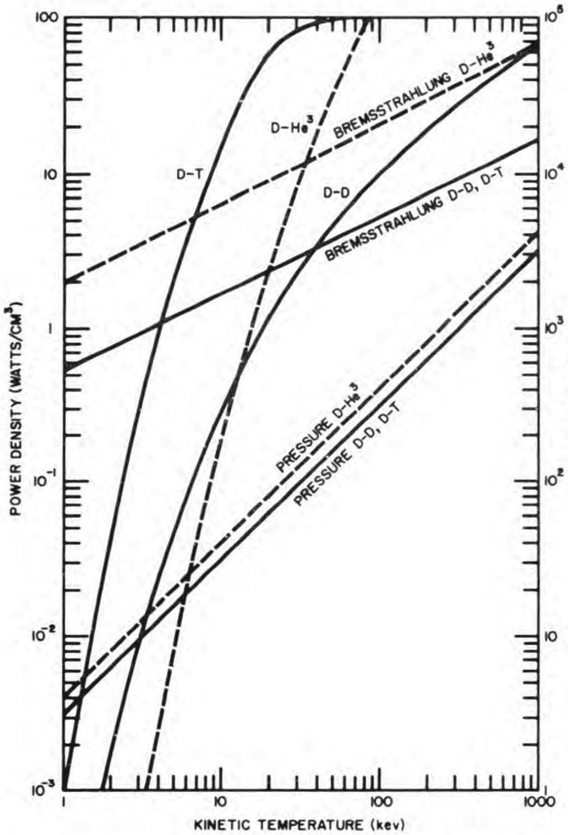

Figure 4 — Fusion reactions, bremsstrahlung losses and the ideal ignition temperature

high atomic number, must be rigorously excluded from the reacting plasma of a fusion reactor.

Suppose it is known how to produce a D-D, D-T, or D-He^3 plasma at a temperature greater than the ideal ignition temperature. How is such a plasma to be contained free of the chamber walls and what is the required field strength? As stated earlier, a magnetic field is the principal candidate for containment. The magnetic field strength required depends on the power density desired and the required particle density to obtain this power level. Power density for the D-T, D-D, and D-He^3 reactions as a function of fuel nuclei density are given in Figure 3 for an estimated operating temperature of 100 kev. A power level of 100 watts/cm^3 is shown which corresponds to power density of a typical fission reactor. This power density gives a fuel density of 10^{15} to 10^{16} nuclei/cm^3. On the other hand, the particle density can be related to the strength of the magnetic field B required through the parameter

$$\beta = \frac{nkT}{B^2/8\pi} \qquad (4)$$

which is the ratio of the contained plasma kinetic pressure to the confining magnetic field pressure. Although plasma stability requirements may specify β to be less than unity, Equation (4) may be used to indicate the order of magnitude of the field required to contain a fusion plasma. The plasma kinetic pressure is given as nkT where n is the total particle density (ions and electrons) and k is Boltzmann's constant. Taking n as 2×10^{15} particles/cm^3 (D-D, D-T plasmas) and n as 2.5×10^{15} particles/cm^3 (D-He^3 plasma) at a temperature T of 100 kev, a magnetic field B of approximately 90,000 gauss for D-D or D-T plasmas and about 100,000 gauss for D-He^3 plasmas would be required for containment. Magnetic fields of this order are not outside the realm of practicality, provided the dimensions of the containing chamber are not too large. It was mentioned earlier that particle densities in the vicinity of 10^{15} nuclei/cm^3 corresponded to only a fraction (10^{-5}) of atmospheric particle density. Still, at the temperatures required for a fusion reactor, this results in a pressure many times atmospheric which must be contained by the magnetic field. The containment pressures for the plasmas of interest as a function of their kinetic temperature are shown in Figure 4. As a result of these low particle densities, a distinct advantage for the envisioned fusion reactor is acquired. The low particle density means that the mass density of the fusion fuel is about 7 to 8×10^{-8} grams/cm^3; therefore, the energy content of a fusion reactor would not be large even at high operating temperatures. In view of this, the explosive hazard of such a reactor would be negligible.

To provide containment, how does a magnetic field influence the motion of the plasma particles? In a uniform magnetic field, the ions and electrons gyrate in opposite directions around the magnetic lines of force as shown in Figure 5. If the particle has no motion parallel to the magnetic field, the motion will be a circular path. With motion parallel to the field, the path will be spirals along the field lines with the magnetic field influencing only the circular motion. The angular frequency ω_c for charged particles in a magnetic field is given as

$$\omega_c = 1.6 \times 10^{-20} \frac{BZ}{m} \text{ radians/sec} \tag{5}$$

where B is the field strength in gauss, Z is the particle charge or atomic number (1 for an electron or hydrogen isotopes) and m is the mass of the particle in grams. This frequency is generally known as the cyclotron frequency. Applying energy to the plasma at the ion or electron cyclotron frequency is included as a technique to heat the plasma. The radius of gyration or the cyclotron radius r_c is determined by

$$r_c = 3.3 \times 10^{15} \frac{(mT)^{1/2}}{ZB} \text{ cm} \tag{6}$$

with m, Z, and B in units used for Equation (5) and T is the particle temperature in kev assuming the particle velocity distribution is Maxwellian. Equations (5) and (6) show that increasing the magnetic field strength (increasing field line density) increases the cyclotron frequency

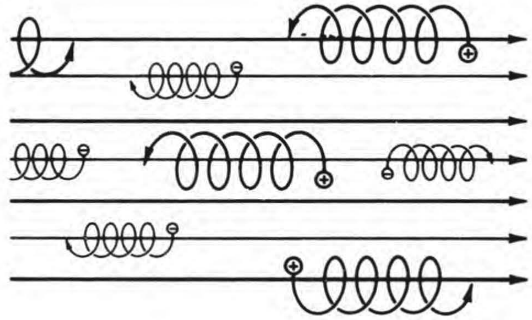

Figure 5 — Plasma particle paths in a magnetic field

ω_c and decreases the cyclotron radius r_c. At a temperature of 100 kev and field strength of 100,000 gauss, r_c is 0.01 cm and ω_c is 1.75×10^{12} radians/sec (2.8×10^{11} cycles/sec) for an electron or 0.60 cm and 4.8×10^8 radians/sec for the deuteron. Ideally, the charged particles in a magnetic field may be considered stuck to a line of force. The ions and electrons will collide and, after each collision, the center of gyration can shift to a neighboring field line. After a large number of collisions, particles can migrate to the wall of the container where they will lose their energy. This process, called classical diffusion, is not regarded as a serious cause of leakage because, at the high temperatures required, the ion-electron collision rate is relatively low. Also, classical diffusion rate is inversely proportional to the square of the magnetic field strength.

This is only a sketch of essentially single particle motion in a uniform magnetic field. For experimental situations in a chamber of 10^{15} high temperature particles/cm^3, the resulting magnetic field will be time and space varying due to the coupling with the particles and their associated microscopic and macroscopic electric fields. Under these conditions, the resultant particle motion, energy transport, diffusion phenomena, *etc.* become extremely complex.

In general, there are two means utilized to generate a magnetic field for plasma containment. A current within the plasma can generate its own magnetic field, or a current external to the plasma can generate the magnetic field. Sketches of these fields are shown in Figure 6 for a toroidal geometry. The well-known pinch effect is the self-constriction

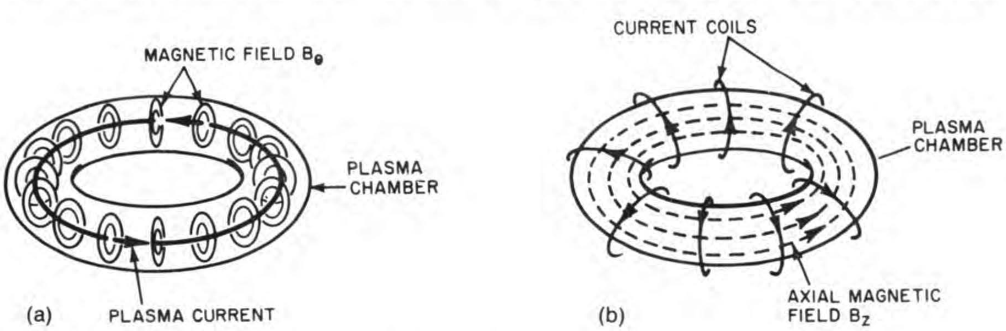

Figure 6 — Magnetic fields: (a) Generated by an induced plasma current, (b) Generated by external current coils (see Ref. 4)

424-809 O - 71 - 2

that occurs in a plasma as a result of a unidirectional current as shown in Figure 6a. The azimuthal magnetic field B_θ serves to confine, compress and heat the plasma. However, the simple pinch is an example of a magnetic confinement scheme which is susceptible to hydromagnetic instabilities. Two distortions of a pinched plasma, the kink and the constriction are shown in Figure 7. It takes only a few microseconds for a kink or constriction to develop in a pinch plasma experiment. Once either of these instabilities start to develop, their growth rate is such that the plasma column is lost to the chamber walls within a few microseconds.

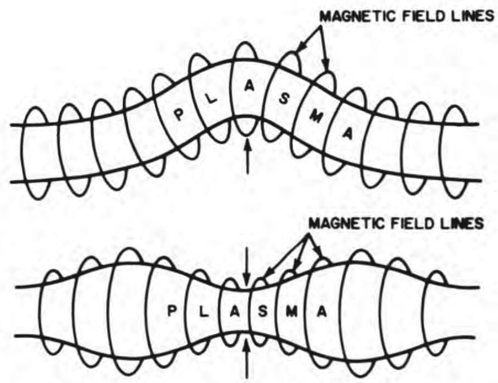

Figure 7 — Instabilities in a pinched plasma (see Ref. 4)

One technique used to increase the stability of the pinch is to add a magnetic field parallel to the plasma axis. Essentially, this is using both fields shown in Figure 6 in the same experiment. The axial field B_z is generated first, then the current in the plasma develops the azimuthal field B_θ which traps some of the axial field in the plasma column. This technique increases the stability of the pinch. However, other pinched plasma instabilities are not affected by the axial magnetic field and adequate containment is not accomplished.

The fields generated by the plasma current and those generated by currents exterior to the plasma provide 14 or so different magnetic field geometries being utilized to study high temperature plasma containment. In addition to a containment scheme, a method must be devised to heat the plasma. Up to temperatures of about 0.5 kev, a fusion plasma can be heated by passing an electric current through it. This procedure is called ohmic heating since it depends on the resistance of the medium carrying the current. The resistivity of a plasma is inversely proportional to the temperature of the plasma. Consequently, as the temperature increases, the plasma resistivity decreases and ohmic heating becomes ineffective above plasma temperatures of about 0.5 kev. In some plasma experiments, ohmic heating appears to result in plasma temperatures greater than a kev. This heating is attributed to turbulent resistivity of which the physical details are not understood. Other heating techniques include magnetic field compression, magnetic and hydrodynamic shock waves, ion and electron cyclotron resonance, radio frequency waves and laser beams. Each or any combination of these heating techniques must be coupled with a containment mechanism.

The qualitative description of the microscopic behavior of ions and electrons coupled with a magnetic field and the macroscopic behavior of the plasma in the simple pinch gives some insight as to the complexity of magnetic confinement of a high temperature plasma. At this time, it is possible to heat plasma densities of 10^{15} ions/cm^3 to temperatures greater than the ideal ignition temperature. However, the confinement time of such plasmas have been no more than a few millionth of a second compared with a tenth of a second or so to be the minimum needed for a pulsing fusion system. At very low plasma densities, confinement times in terms of minutes have been realized; the problem here is to build up the density without jeopardizing confinement. In general, the limitations so far have been an understanding of the physics of high temperature plasmas and their interaction with electromagnetic fields.

In studying the behavior of magnetically confined and heated plasmas, techniques must be devised to determine the microscopic plasma properties such as temperature, pressure, electron and ion densities, electron and ion energies, electric and magnetic field distributions, current strength, and extent of fusion reaction. The experimental procedures used to obtain such information are referred to as plasma diagnostic techniques. The complexity of electromagnetic plasma interactions is such that considerable ingenuity is required to apply these techniques and to interpret the results of the measurements made. A few of the plasma properties that are studied and some of the methods employed are summarized in Table II. Detailed explanations of these procedures are beyond the scope of this article, but the listing indicates the complexity of plasma research and the variety of equipment and techniques in use.

TABLE II
Plasma Diagnostic Techniques (Refs. 5 and 6)

Quantity Measured	Diagnostic Method
Ion density and distribution	Optical spectroscopy; electrostatic probes; electron beam scattering
Ion energy	Optical spectroscopy; fusion reactions; mass spectroscopy
Electron density and distribution	Microwave and optical interferometer; light scattering; optical spectroscopy
Electron energy	Light scattering; X-ray emission; optical spectroscopy

TABLE II (Continued)

Quantity Measured	Diagnostic Method
Magnetic field distribution	Magnetic probes; optical spectroscopy
Electric field distribution	Light scattering; optical spectroscopy
Plasma current	Inductive current shunts; current transformers
Plasma pressure distribution	Magnetic probes; piezoelectric crystals
Turbulence and instabilities	Electron and ion beam scattering; light scattering; optical spectroscopy
Neutron emission	Boron counters; scintillation detectors; silver foil activation
Neutron energy	Track plates; cloud chambers

Fusion Research

At this point, the general physical parameters for a controlled fusion reactor have been outlined with a sketch of the experimental complexity to attain these plasma conditions. The approximate plasma parameters are summarized as follows:

Plasma Constituents		- D, T, He^3
Minimum Ignition Temperature	D-T	- 4 kev
	D-D	- 36 kev
	D-He^3	- 34 kev
Ion Density		- 10^{15}-10^{16} ions/cm^3
Operating Kinetic Temperature		- 100 kev
Magnetic Field		- 90,000 to 100,000 gauss

As shown in arriving at these general parameters, they are typical conditions which appear to be necessary for a controlled fusion reactor. A survey of controlled fusion research indicates that the plasma parameters under investigation cover a broad range compared with the above list of approximate plasma conditions. Some of the reasoning for this is that plasma physics is still in its infancy as a science as well as the fact that a wide range of plasma parameters must be traversed to arrive at the desired reactor conditions. Coupled with the research to understand basic plasma properties is the research to understand the behavior of magnetically confined high temperature plasmas. Here again, there are a number of different approaches, but basically, the approaches differ in the geometry of the magnetic field for confining the plasma. In view of the wide range of plasma parameters and the variety of magnetic field geometries, this article will briefly summarize one of the simpler geometries – the Tokamak 3. The Tokamak 3 experiments are conducted at the I. V. Kurchatov Institute in Moscow. Besides having one of the simpler magnetic confinement geometries, this is one of the fusion experiments which has attained relatively high temperature, density and containment at this time.

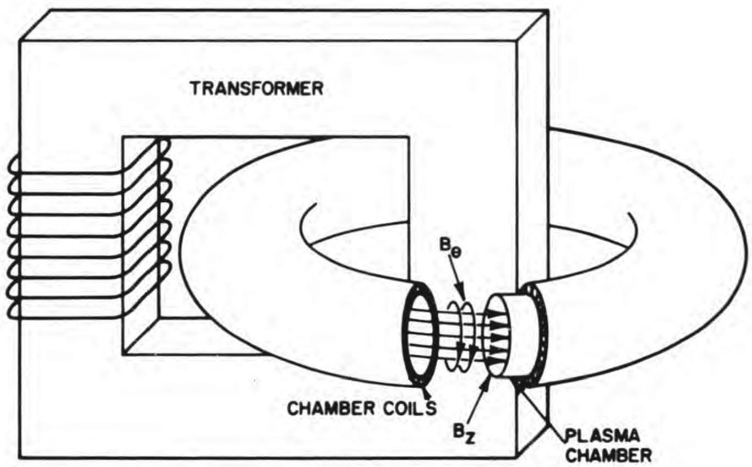

Figure 8 – Tokamak 3 sketch

A sketch of the physical geometry for the Tokamak 3 is shown in Figure 8. It has a doughnut shaped or toroidal plasma chamber with an overall diameter of two meters and a chamber diameter of 30 centimeters. The magnetic field for plasma confinement and heating is a composite of two separate fields. These two fields are illustrated in Figure 6. The toroidal field B_z is formed by a current flowing through coils wrapped around the outside of the plasma chamber. The magnetic field B_θ is in an axial direction around the minor axis of the torus. This field B_θ results from the induced plasma current – the plasma acts as a secondary of the transformer. The magnetic fields produced in the plasma chamber are additive, but since the two are perpendicular to each other, the resultant field is on the bias. This twisting or helical magnetic field tends to confine and stablize the plasma. Current through the plasma not only contributes to the helical field but also heats the plasma through an ohmic or resistance heating process. In other high current experiments, ohmic heating of a confined plasma has been limited because the resistivity is inversely proportional to the plasma temperature. The particular set of current parameters used in the Tokamak experiments have given rise to certain areas of turbulent resistivity which appears to account for the additional heating through the ohmic process. At this time, not all of the physical reasons for the formation of the helical confining field and how the turbulent heating is accomplished are understood.

The reported Tokamak 3 results are:

Electron temperature	(T_e)	$\sim$1 kev
Ion temperature	(T_i)	$\sim$0.5 kev
Confinement time	(τ)	$\sim$0.02 sec
Density	(n)	$\sim 2\text{-}5 \times 10^{13}/\text{cm}^3$

The generally accepted parameters for a true D-T fusion plasma are $T \sim 10$ kev and a combination of density and confinement time such that the product $n\tau$ is equal or greater than 10^{14} ions-sec/cm^3. These parameters are called the "Lawson Criteria" and is usually referred to as a dimensionless term with the understanding that n is in ions/cm^3 and τ in seconds. The calculated maximum $n\tau$ from the Tokamak 3 results is 10^{12}. An order of magnitude increase in each of the three parameters (T, n, τ) could result in a true D-T fusion plasma or proof of fusion power feasibility. Fusion power feasibility can be defined as—more convertible fusion energy out of the system than is required to promote the fusion reactions. Using $n\tau$ as a general criteria of controlled fusion progress, a $n\tau$ of about 10^{10} was the best that had been accomplished in a toroidal geometry since 1956 until the Tokamak results were reported at the International Atomic Energy Association meeting in 1968.

The results of the Tokamak program represent over 15 years of worldwide theoretical and experimental research with high temperature plasmas and their interactions with electromagnetic fields. These efforts were directed toward understanding the fourth state of matter—plasma—as it may apply to a controlled fusion power plant. In the first theoretical plasma models, the plasma was treated as two interpenetrating fluids—one composed of positively charged particles and the other of negatively charged particles. Devices built on the basis of this model lost their plasma much more rapidly than theory predicted. Later experiments showed that a number of loss mechanisms or instabilities were responsible. Since the plasma behavior is much more complex than the first theoretical models indicated, the controlled fusion program has broadened its research base. For some time experimental devices have been built which may not be suitable for the ultimate fusion system but do enable researchers to study plasma behavior at the microscopic level. At this time, there are approximately 115 major plasma experiments in the world and they utilize 14 different magnetic field geometries. Of the 14 magnetic field configurations, only about four have a reasonable chance of being developed into a controlled fusion reactor. Consequently, the complexity of plasma behavior is well known and the worldwide effort is directed toward an increased knowledge of plasma-electromagnetic field interactions.

The names of the experimental devices with the location of major fusion experiments are listed in Table III. Each listed nation will have one or more plasma experiments with the total for all nations being

Table III
Location of Major Controlled Fusion Experiments (Ref. 7)

	Device Name	Experiment Locations
Closed Configurations	Astron	US
	Floating Rings	France, Germany, Japan, Sweden, UK, US
	Heliotron*	Japan
	RF† Interaction	USSR
	Stellarator‡	France, Germany, Japan, UK, US, USSR
	Tokamak‡	Australia, Japan, US, USSR
	Toroidal Screw Pinch	Netherlands, USSR
	Toroidal θ Pinch‡	Germany, France, UK, US
	Toroidal Z Pinch	France, UK, USSR
Open Configurations	Cusps	Poland, USSR
	Linear θ Pinch	France, Germany, Italy, Japan, UK, US
	Linear Z Pinch	Italy, UK, US, USSR
	Magnetic Mirrors‡	France, Japan, UK, US, USSR
	RF† Interaction	USSR

*Toroidal Picket Fence Geometry
†Radio Frequency
‡Possible Fusion Reactor Configurations

about 115. The four device configurations which may develop into a fusion reactor are marked in Table III. The geometries are listed as closed and open configurations. A closed magnetic field configuration is of the Tokamak type where the magnetic field (or fields) closes on itself in the plasma chamber. The open configuration is usually a straight cylindrical plasma chamber with magnetic stoppers at the ends. A magnetic mirror system is an example of an open configuration as shown in Figure 9. Magnetic stoppers are formed at the ends by the high concentration of field lines which tend to reflect the plasma particles back into the central region. For a detailed description of the named devices in Table III, see References 1, 2, 3, and 7 at the end of this article.

In the United States there are four major plasma physics laboratories; Oak Ridge National Laboratory, Princeton Plasma Physics Laboratory, Los Alamos Scientific Laboratory, and Lawrence Radiation Laboratory. These laboratories are directed at the AEC. In addition, about 40 universities, a number of industrial laboratories and several government laboratories have small plasma physics programs. A major portion of the United States controlled fusion research is sponsored by the AEC. The National Science Foundation, Air Force Office of Scientific Research

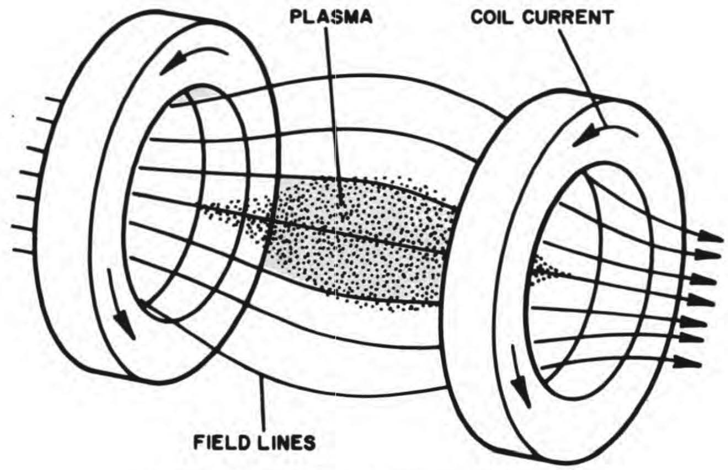

Figure 9 – Magnetic mirror sketch

and the Office of Naval Research sponsor fusion research as it relates to their mission.

In the fusion reactions are implicit new dimensions—those of power obtained by direct electrical conversion from an inexpensive, safe and virtually inexhaustible fuel. These possibilities could play a dominant role in shaping not only the world energy picture but also the Navy's operational capabilities of the future. With all projections indicating that naval ships and fixed installations will require increasing amounts of power to meet future operational requirements, it is essential that Navy research consider the capabilities and limitations of all power sources, including fusion. This article reviews the current status of research in fusion power and shows the advances required to bring this means of power production to a demonstration of feasibility.

References

1. S. Glasstone and R. H. Lovberg, *Controlled Thermonuclear Reactions,* D. Van Nostrand Co., Inc. (1960)
2. D. J. Rose and M. Clark, Jr., *Plasma and Controlled Fusion,* M. I. T. Press and John Wiley & Sons Inc. (1961)
3. L. A. Artsimovich, *Controlled Thermonuclear Reactions,* Oliver and Boyd Ltd. (1964)
4. S. Glasstone, *Controlled Nuclear Fusion,* USAEC Technical Information Division (June 1964)
5. H. R. Griem, *Plasma Spectroscopy,* McGraw-Hill Book Co. (1964)
6. M. A. Heald and C. B. Wharton, *Plasma Diagnostics with Microwaves,* John Wiley & Sons Inc. (1965)
7. A. S. Bishop, *World Survey of Major Facilities in the Field of Controlled Fusion,* USAEC, Washington, D.C. (November 1969)

Bibliography

R. F. Post, Controlled Fusion Research, *Reviews of Modern Physics,* Volume 28, Number 3, page 338 (July 1956)

L. Spitzer, Jr., *Physics of Fully Ionized Gases,* Interscience Publishers, Inc., Second Edition (1962)

Thin Film Coatings by Sputtering

James Comas
Naval Research Laboratory

Introduction

The technological applications of thin film coatings range from household goods to sophisticated electronic devices. There has been a continual development of coating techniques and a great deal of effort has been expended in the development of equipment to keep abreast of the increasing demands of industry and research. Some areas that are receiving special attention at present in the thin film field are: protective layers for passivation and radiation shielding, reflecting and partially reflecting surfaces, and the fabrication of a wide variety of electronic devices. Research results in the thin film coating field have even been applied to the development of a razor blade which has a platinum chromium alloy thin film which is claimed to greatly increase the life of the shaving edge.

The objective in thin film coating is to transport onto a sample a thin layer of material. For most applications thicknesses in the order of several thousand atomic layers are sufficient. There are two techniques currently used to accomplish this. One is "vacuum evaporation" and the other "sputtering."

In the vacuum evaporation technique, the coating material (*e.g.*, silver) and the object to be coated are placed in a vacuum chamber. The coating material is heated, and the particles which evaporate from it collect on the object (and elsewhere in the chamber). The thickness of the film deposited can be monitored by several standard optical and electronic techniques. The formation of film coatings by the evaporation of metals whose melting temperatures are of the order of 1000°C (*e.g.*, copper, silver, gold) is a routine procedure and many samples can be processed in the same chamber simultaneously.

The sputtering studies performed at the University of Delaware by the author have been continued by him at the Naval Research Laboratory, where the work has been extended to include a wide variety of bombarding particles and materials which will provide important new applications for the Navy.

**Dr. Comas* received his PhD and MS in physics from the University of Delaware. The first two years at the Naval Research Laboratory were as an National Research Council Postdoctoral Research Associate, during which time his research emphasized sputtering, silicon oxidation, and low energy ion-plantation studies. At present he is in the Electronics Division working primarily on ion-implantation of semiconducting materials.

Although at present there are numerous applications for coatings by evaporation, there are an increasing number of areas where this technique is not well suited. One of growing interest is the formation of thin alloy films with predictable composition and characteristics. The formation of a thin alloy film by evaporation is very difficult since in most cases the source material will not evaporate and deposit stoichiometrically; that is, the material condensed on the substrate will not have the same composition as the source. Simultaneous evaporation from separate sources to obtain the proper alloy composition is difficult due to the different vapor pressures of the materials involved. Another major difficulty is that rather high temperatures and a controlled environment are required for the formation of thin insulating films, *e.g.*, quartz and aluminum oxide, by evaporation. Similar high temperature problems occur in making thin films of the refractory metals.

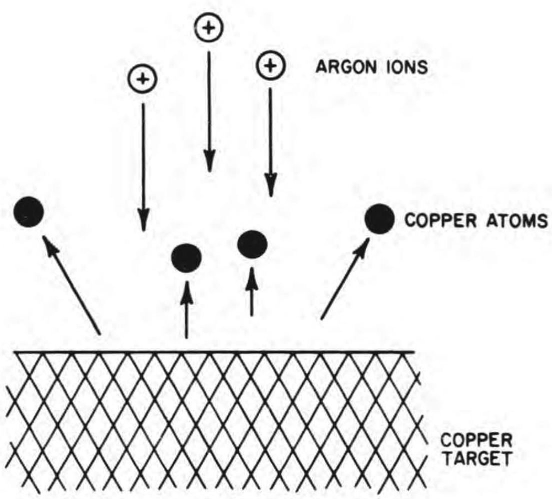

Figure 1 — Schematic diagram of the sputtering of a copper surface by a beam of energetic argon ions. The particles ejected as a result of the argon-copper collisions leave the surface primarily as neutral atoms of copper.

The above difficulties led researchers to reconsider sputtering which, until recently, was considered inferior to the evaporation technique and little used. Sputtering is the erosion of a surface that is subjected to energetic gas bombardment. Figure 1 shows schematically the sputtering of a copper surface by a beam of energetic argon ions. As a result of the collisions by the incoming beam, surface atoms are ejected. The rate at which the surface is removed depends on the energy and mass of the incoming particle and the physical properties of the target. The object to be coated is placed in a position so it is in the path of the beam of material sputtered from the target surface. Film thicknesses can be controlled by the intensity and energy of the bombarding beam, substrate position, and sputtering time.

The first known report on sputtering appeared in the Transactions of the Royal Society in 1852 and was by W. R. Grove (1). He observed the erosion of the cathode material in his glow discharge experiments. Later, thin films were deposited by sputtering, but such films were of poor quality and the technique was abandoned in favor of the vacuum evaporation technique until the 1950's when the special needs of microelectronics arose. Since then, not only have the technical aspects of the process been developed, but also considerable effort has been directed toward increasing our knowledge of the underlying physics. In particular, there has been a gain in our understanding of the ejection process and of the nature of the interaction between the surface atoms of the target and the incident particles.

Apparatus

There are several methods to obtain energetic ion beams for sputtering studies and coating experiments. One method is to obtain the beam from a mass spectrometer system. This gives well resolved beams in the KeV range, but usually of low intensity ($\mu A/cm^2$). Another method is to place a metal target which is negatively biased in a plasma (essentially as a Langmuir probe). A plasma is a region of positive ions and electrons and is generated by ionizing the atoms of the bombarding species, *e.g.*, argon. This method gives high intensity (milliamperes per cm^2, mA/cm^2) and low energy (below KeV) beams. An eV is equal to an electron volt and a KeV is a thousand electron volts. For most deposition and coating experiments the Langmuir probe method is the most convenient because of its simplicity and the high sputtering rates that can be obtained.

The method of extracting a beam from a plasma or using an analyzed beam from an accelerator works well on materials that are conductors. However, if an insulator is bombarded with a dc positive ion beam a surface charge accumulates (since it cannot be conducted away). A positive surface potential is soon reached, repelling the incident ion beam and the surface ceases to be sputtered. The charge build-up can be avoided if an electron beam is scanned over the surface so that charge neutralization takes place on the surface. A more practical method is to apply a radio frequency (RF) potential to the target which bombards the surface with electrons in the positive cycle so that the surface is periodically neutralized. This technique is called *RF Sputtering* and was first suggested by G. K. Wehner in 1955 (2,8). The interest in insulating and semiconducting thin films is such that at present most major vacuum equipment companies are marketing RF sputtering apparatus.

A Langmuir probe sputtering arrangement is shown in Figure 2. The apparatus is placed in a bell jar vacuum system which has a base pressure of 10^{-6} mm of mercury (torr) or better. An inert gas is bled continuously into the system through a leak valve to a pressure of about

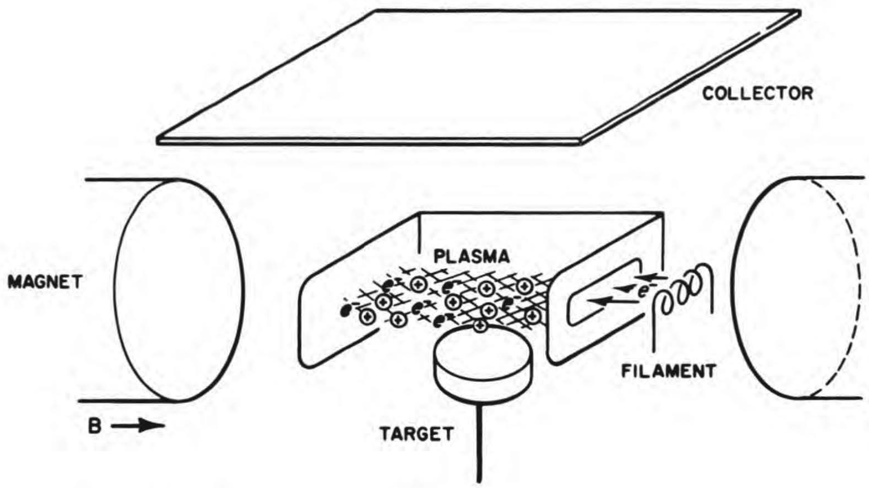

Figure 2 — Diagram of a DC sputtering apparatus using the target as a Langmuir probe. The target is placed about 2 mm beneath the plasma region. Positive ions are drawn out of the plasma region and bombard the target when it is negatively biased with respect to the plasma. The sputtered material travels through the plasma region and deposits on the collector.

1×10^{-3} torr. Electrons are emitted from the filament and are drawn into the ionization chamber through a slit in the chamber. A magnetic field along the slit-filament alignment helps confine the electron beam. Under proper operating conditions a thermionically sustained, magnetically confined, arc discharge is struck in the chamber. The target, placed in the chamber just below the electron beam, is bombarded with positive ions drawn from the discharge when it is biased negative with respect to the discharge. Bombarding ion beams in the order of $10 mA/cm^2$ can be obtained with such an arrangement; however, the energy is usually limited to below 1 KeV. An important consideration is that the target-collector distance be less that the mean free path at the pressure at which the bombardment takes place.

A schematic diagram of an RF sputtering apparatus is shown in Figure 3. The apparatus is placed in a bell jar vacuum system (with proper RF shielding) with a base pressure of 10^{-6} torr or better. An inert gas is bled into the system, usually to about 10×10^{-3} torr. The target holder is water cooled because of the heat produced by the RF bombardment. A plasma is generated by the application of an RF potential to the target, which is capacitively coupled to the plasma. If the target is a metal, a series capacitor must be inserted in the target leg. On the negative cycle positive ions are drawn from the plasma region and bombard the target. The sputtered particles travel across the plasma region onto a substrate placed opposite the target. On the positive cycle electrons are drawn from the plasma and neutralize the charge that has accumulated from the positive ion bombardment. The RF

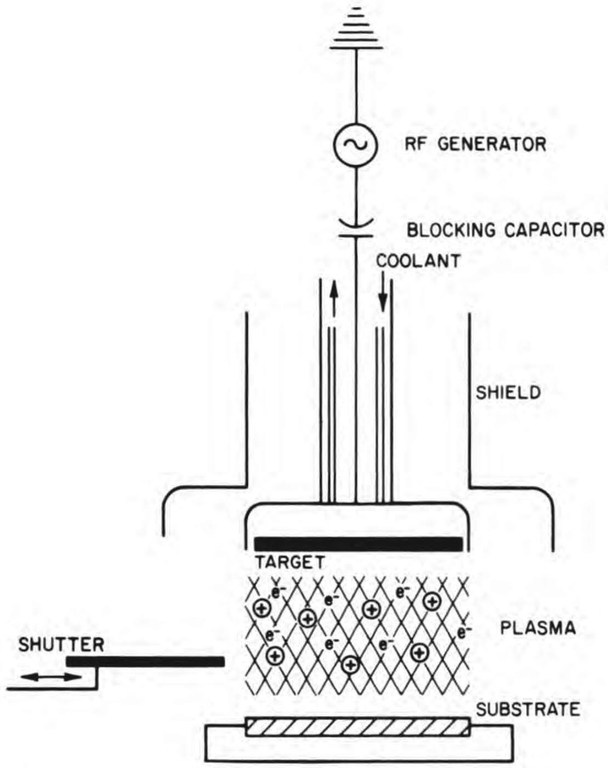

Figure 3 — Diagram of an RF sputtering apparatus. The RF frequency applied to the target is usually around 10-20 MHz, with peak-to-peak voltages around 4000 volts. On the negative cycle positive ions are drawn from the plasma and sputter the target. On the positive cycle electrons are drawn from the plasma and neutralize the charge that has accumulated from the positive ion bombardment. The sputtered material deposits on a substrate placed as shown. Insulating materials, such as quartz and aluminum oxide, can be sputtered using the above arrangement.

frequency used is in the megacycle range, usually around 10 to 20 MHz, with peak-to-peak voltages around 4000 V. By using RF sputtering, insulating materials such as quartz and aluminum oxide can be put onto substrates at a rate of 1 to 2 thousand angstroms per minute.

Physical Sputtering

On entering the surface of a solid an incident energetic particle in the kilovolt range will lose its energy by collisions with atoms in the solid. After a series of collisions, in which atoms in the solid are displaced from their normal sites, the incident particle will come to rest and be trapped. One of the results of the bombardment is the ejection of atoms from the surface of the solid. The ejection of particles from a surface subjected to massive particle bombardment is one of the more pronounced manifestations of the bombardment process. Although the sputtering of metallic solids has been studied extensively for many years, the sequence of events that lead to the ejection of a surface atom has not yet been clearly established. The purpose of this section is to present the important features and the experimental parameters involved in the technological and basic aspects of sputtering.

Sputtering is divided into two categories; physical sputtering and chemical or reactive sputtering. Physical sputtering occurs when the ejection process is caused by a series of elastic collisions and there is no chemical interaction between the incident particles and atoms of the target. Experimentally the bombarding particles in most physical sputtering studies are noble gas ions. The number of particles ejected per incoming bombarding ion in physical sputtering is a function of the mass and energy of the incident ion.

Chemical sputtering occurs when the bombarding particles interact with surface atoms and the ejection is not due solely to elastic collisions. In chemical sputtering, ejection can occur even though the incident energy of the ions is below the threshold or minimum energy needed for physical sputtering. Hydrogen ions, for example, will form volatile compounds when bombarding a metal surface.

The incident ions are neutralized at the surface by electrons from the metal. Most sputtering experiments are performed at bombarding energies in the low KeV range. The bombarding particles enter the surface and lose their energy through elastic collisions with the target atoms. If a surface atom receives sufficient energy in the proper direction it can be ejected. The ejected atoms leave the surface as shown in Figure 1, and can be collected by placing a substrate (such as a glass slide) above the target.

Experimental Parameters

Some of the main parameters to be considered in sputtering experiments are:

- sputtering yields,
- mass analysis of the sputtered particles,
- chemical composition of the deposits formed, and
- the direction of ejection of the sputtered material.

Many of the salient properties of the sputtering phenomenon can be obtained from studies made on polycrystalline metallic materials. Much of the recent work, however, has been focused on the sputtering of single crystals because of the important effects that are dependent on the structure of the target.

The sputtering yield is defined as the number of particles ejected from a surface per incoming ion. The yield can be written as,

$$Y = \frac{N_a}{N_b} = \frac{W(0.965 \times 10^5)}{I\,T\,A}$$

where N_a = number of sputtered atoms
N_b = number of incident ions
W = weight loss of the target in grams
I = ion current to the target in amps
T = sputtering time in sec
A = mass of the target atoms in atomic mass units.

The most direct method to calculate the yield is to weigh the target to obtain the weight loss due to the bombardment; the total charge, $I\,T$, can be measured directly with a current integrator. For high yield materials the sputtering time must be of the order of hours to obtain reliable results by weighing. Many sensitive methods have been developed to measure yields, especially in the low energy range: spectroscopic, radioactive, and mass spectrometric are some techniques which have been used over the last few years. Quartz crystal oscillators and *in situ* micro-balances have also been used to obtain yield data.

In the sputtering range, the yield increases with increasing bombarding energy. The threshold is defined as the energy below which sputtering does not occur. Experimentally it is difficult to measure yields in the threshold region because of the very small amounts of material sputtered. [Values in the 15 to 35 eV region are given for most metals bombarded by noble gases. From the threshold the yield increases over several orders of magnitude up to the hundred eV range. For example, Cu bombarded at 25 eV with argon the yield is $Y = 10^{-4}$ Cu atoms/Ar^+, the yield rapidly increases to $Y = 1$ for an argon energy of 180 eV (Refs. 3 and 4). In the 5 to 15 KeV range the yield increases less rapidly and reaches a plateau in the 20 KeV range. For an argon-copper interaction, the yield starts to decrease slowly above 20 KeV, where it has reached a value of $Y = 6.80$ Cu atoms/Ar^+, as shown in the yield curve in Figure 4 (Ref. 5).]

The variation in yield with bombarding energy is related to the penetration depth of the incident ions. At low energies the incoming ions lose their energy within a few atomic layers of the surface. As the bombarding energy is increased, especially beyond the plateau region, the penetration depth increases to hundreds of angstroms beyond the surface. Energy losses, therefore, take place far enough beyond the surface with the result that there is a reduction of the energy available at the surface for the sputtering process.

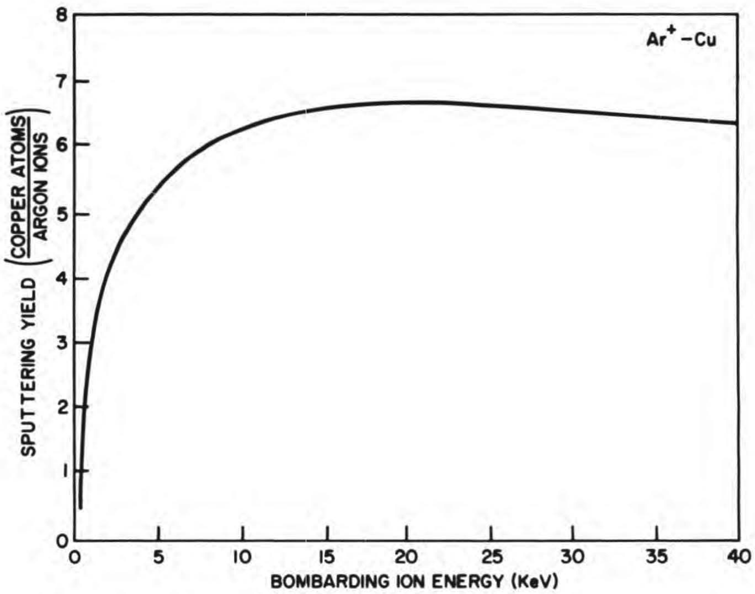

Figure 4 — Sputtering yield curve for argon ions bombarding polycrystalline copper. Data from Ref. 5.

Sputtering yields are affected by the condition of the surface of the target and the vacuum conditions under which the sputtering takes place. One important criterion is that the surface erosion rate far exceed any influence that residual gases in the vacuum system might have. Aluminum, for example, has a very tenacious oxide that is very difficult to sputter. If the removal rate of aluminum by sputtering does not greatly exceed the oxide formation, which would occur from the residual oxygen in the vacuum, the yield measured would be far below the ideal aluminum (Al) value. Yields depend also on the ion-target combination. Metals with closed electronic shells, *i.e.*, Cu, Ag, and Au, have the highest yields since they best approximate hard spheres.

The interactions between the incident noble gas atoms and the target atoms can be viewed as elastic collisions between hard (billiard ball like collisions) spheres. From the conservation of energy and momentum, the maximum energy transferred in a head-on collision is,

$$E = \frac{4E_o\, M_t\, M_i}{(M_t + M_i)^2}\,.$$

Here, E_o is the incident ion's energy, M_t and M_i are the masses of a target atom and the incident ion, respectively. If the masses are equal, the maximum energy will be transferred in the collision. To obtain the highest sputtering yield the masses must therefore be as close as possible.

A mass spectrographic analysis of the sputtered material is important in developing a model to explain the phenomenon and in the deposition of thin films. Experiments have been performed to determine the charge, mass and velocity of the ejected species. It was found that for metals more than 99 percent of the ejected particles leave the surface as neutral atoms. From mass spectrometric studies it was found that GaAs was stoichiometrically sputtered (Ref. 6). An x-ray fluorescence analysis of the deposition from sputtered gallium arsenide (GaAs) showed that the composition of the film collected was the same as the target.

The velocity of sputtered atoms is quite high compared to atoms emitted from a surface thermally. The velocities of sputtered atoms from Cu subjected to Hg^+ bombardment from 150 to 600 eV have been measured by a spectroscopic technique. The velocity distribution was found to be Maxwell-Boltzman with the maximum number ejected at 4.0 eV (Ref. 7).

The distribution of material sputtered from a polycrystalline metal target has a cosine-like distribution. As the bombarding energy is increased the distribution becomes more peaked toward the normal to the surface. When single crystals are subjected to noble gas bombardment the surface atoms are sputtered in preferred directions. The direction of ejection from a crystal depends upon the crystallographic orientation of the target. From observations of the sputtered material on collector substrates it is seen that the emission direction corresponds to the close-packed directions or planes of highest atomic density within the crystal (Ref. 8).

The close-packed directions in face centered cubic (*fcc*) metallic crystals, *e.g.*, copper and silver, are the <110> directions. A schematic drawing of the <110> direction in a *fcc* crystal is shown in Figure 5a. It is along these directions that the sputtering of *fcc* metallic crystals has the highest intensity. In Figure 6a and 6b the sputtered depositions

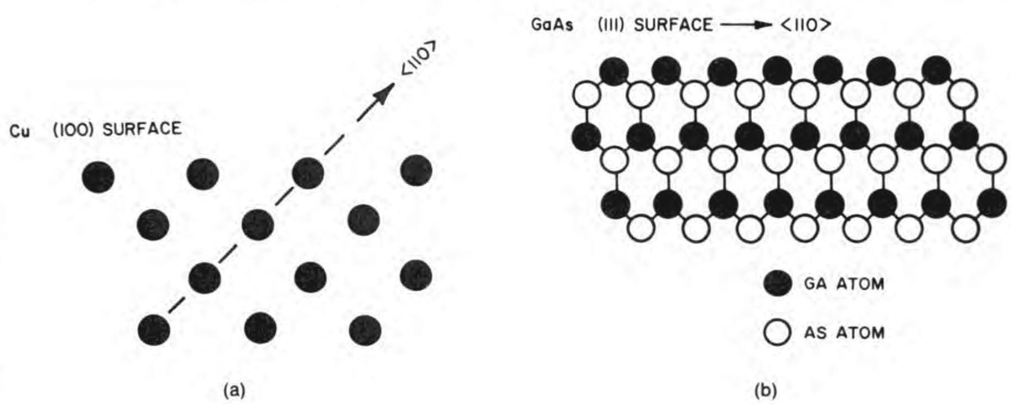

Figure 5 — (a) Schematic drawing of the (100) surface of a fcc crystal (copper). The <110> direction shown makes an angle of 45° with respect to the surface. There are four such close-packed <110> directions leaving the (100) surface at 45° with respect to the surface normal. (b) Schematic drawing of the (111) surface of a zinc-blende crystal (GaAs). The close-packed <110> directions are zig-zagged chains of Ga and As atoms. There are three <110> directions from the (111) surface making an angle of 35° with respect to the surface normal.

are collected on glass slides obtained from the argon sputtering of (100) and (110) Cu crystals. The dense spots correspond to ejection along the <110> directions. GaAs has a zinc-blende structure and the close-packed directions consist of zig-zagged chains of As and Ga atoms as shown in Figure 5b. The dense spots are a result of ejection along the <110> direction. The pattern obtained from a (111) GaAs crystal is shown in Figure 6c.

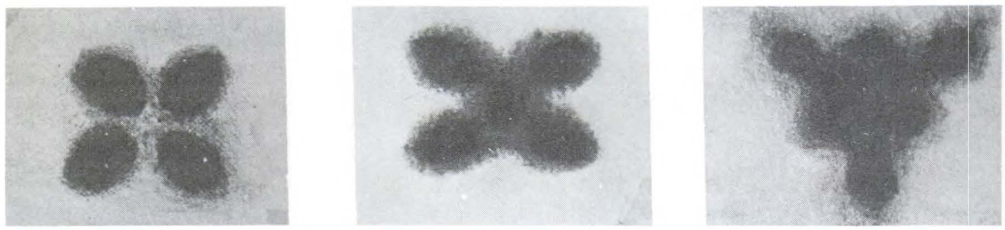

(a) (b) (c)

Figure 6 — (a) Sputtered deposition collected on a glass slide from the argon bombardment of a (100) copper crystal surface. (b) Sputtered deposition collected on a glass slide from the argon bombardment of a (110) copper crystal surface. (c) Sputtered deposition collected on a glass slide from the argon bombardment of a (111) surface of a gallium arsenide crystal surface.

Sputtering Theories

There are essentially two main theories to explain sputtering phenomenon. One theory assumes that there is sufficient penetration depth of the bombarding particle so that the energy from the collision region is transported by the lattice up to the surface. The other assumes that the interactions are confined entirely to the surface layers of the target. Although both approaches predict the spot patterns observed, they are not entirely complete in describing the sequence of events that lead to the ejection of atoms from a bombarded surface.

From lattice structure considerations with respect to radiation damage processes it was postulated that momentum could be focused along a close-packed crystallographic direction (Ref. 9). The fundamental conditions for such focusing are obtained from the geometrical arrangement of the lattice atoms. Figure 7 gives a schematic representation of a focusing collision chain in an atomic row. For focusing to occur the angle θ must become smaller with each successive collision. The mechanism is applied to sputtering by assuming that a localized disturbance is initiated by a bombarding particle through its collision with an atom in a lattice site. The energy of this disturbance is most efficiently drained away along the directions of highest atomic density when a focused collision sequence results. If an atom at the end of a chain receives sufficient energy to overcome its surface binding energy it will be ejected. The closest-packed direction in *fcc* metallic crystals is the <110> and

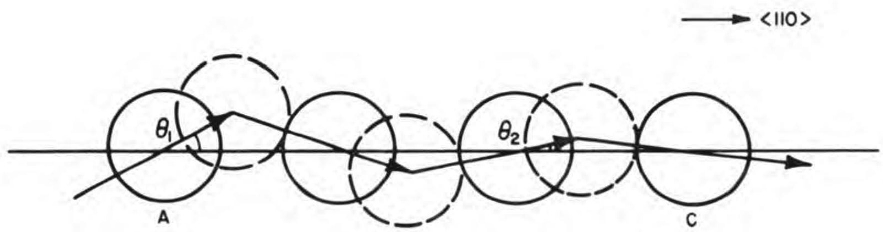

Figure 7 — A schematic representation of a sequency of atomic collisions along a <110> direction. Atom A is struck in such a way that the collisions propagate along the axis of the atomic row. If the angle θ gets progressively smaller ($\theta_1 > \theta_2$) the collisions will be focused along the row of atoms to atom C.

it is along this direction that the sputtered atoms are observed with the highest intensity.

The other approach is to consider the ejection as a result of rebounding or energized particles from the outer surface layers. In the rebounding mechanism a surface atom is driven toward the crystal interior by the bombarding particle. Target atoms in the second layer repel the energetic surface atom and reflect it towards the surface. This rebounding results in the ejection of the surface atom. Computer simulation of such a process has yielded spot patterns which correspond to the experimental observations (Ref. 10). In another surface mechanism proposed the bombarding particle dissipates its energy in such a way that some surface atoms obtain the energy needed to overcome the surface binding energy (Ref. 11). The direction of ejection is obtained from optimum emission paths and energy considerations.

Applications

Sputtering is now used in many laboratories in the preparation of thin films on electronic and optical devices. A great deal of effort has been exerted in the electronics field on the deposition of thin films in the fabrication of microelectronic devices. Refractory metals and insulators that are very difficult to evaporate can be deposited by sputtering. The protection of the surfaces of solar cells used on space craft against radiation is important as the radiation damage decreases the cell's efficiency. Transparent insulating films are deposited on the solar cell surface which protects the surface with a negligible increase in weight. (Wehner has estimated that about 40 meters have been sputtered from the surface of the moon as a result of energetic proton and helium bombardment.)

Etching is an essential step in the fabrication of planar semiconductor devices. Sputtering is being used as an etching technique in removing metallic and insulating layers. The advantages of removing the surface by sputtering are: it leaves no chemical residue; it is easy to mask the section of interest; there is no undercutting at the edges of the etched region; and the etching rates are easily controlled.

Doped thin films can be deposited on substrates by sputtering a target which has the doping content desired. Cermets, which are ceramic-metal mixtures, such as Cr-SiO, $Cr\text{-}MgF_2$, and $Au\text{-}SiO_2$, and are used to form highly stable thin film resistors, are being made commercially by sputtering. It has been found that films made by sputtering have better adhesion and fewer pinhole effects than those formed by evaporation.

References

1. W. R. Grove, *Trans. Roy Soc.* (London) **142,** 87 (1852)
2. G. S. Anderson, W. N. Mayer, and G. K. Wehner, *J. Appl. Phys.,* **33,** 2991 (1962)
3. J. R. Woodyard and C. B. Cooper, *J. Appl. Phys.,* **35,** 1107 (1964)
4. N. Laegreid and G. K. Wehner, *J. Appl. Phys.,* **32,** 365 (1961)
5. G. Carter and J. S. Colligan, *Ion Bombardment of Solids* (American Elsevier, N.Y. 1968). Data taken from Figure 7.3.
6. J. Comas and C. B. Cooper, *J. Appl. Phys.,* **38,** 2956 (1967)
7. R. V. Stuart and G. K. Wehner, Ninth Nat. Vac. Symp., Pergamon Press, N.Y. (1962)
8. G. K. Wehner, *Advances in Electronics and Electron Physics,* Vol. 7, 239 (1955)
9. R. H. Silsbee, *J. Appl. Phys.,* **28,** 1246 (1957)
10. E. Harrison, J. P. Johnson, and N. S. Levy, *Appl. Phys. Letters,* **8,** 33 (1966)
11. C. Lehmann and P. Sigmund, *Phys. Stat. Sol.,* **16,** 507 (1966)

New Monitoring Technique Expected to Save Lives

A new clinical monitoring technique is expected to save lives in cases of wounded men suffering traumatic shock injuries. The development of the technique is a result of studies by Dr. M. Pomerantz at the University of Colorado under an Office of Naval Research contract, with partial support by the Bureau of Medicine and Surgery. The work stems from the situation that men wounded in Southeast Asia are able to be delivered to a hospital by helicopter within a few minutes after an injury is received, making immediate treatment possible. Cases were cropping up, however, where men suffering severe wounds of the extremities were given adequate treatment but then became critical due to lung complications brought on by an increase of fluids in the lungs, known as pulmonary edema. Traumatic injuries are followed by a weakening of the lung functions, a condition that is difficult, and sometimes impossible, to reverse once there is an accumulation of fluids in the lungs. Present methods for monitoring such patients frequently fail to detect the warning sign that lung fluids have started to increase. A reliable measuring device was needed. The Navy was concerned because treatment of traumatic injuries is particularly important in the case of casualties aboard ship.

(Continued on Page 29)

On the Naval Research Reserve

Oceanographer of the Navy Speaks to NRRC 5-9

Rear Admiral William W. Behrens, Jr., USN, Oceanographer of the Navy, spoke on, "The Role of Oceanography in Naval Operations," at the meeting of Naval Reserve Research Company 5-9 held at the Naval Research Laboratory, Washington, D.C. Many laboratory personnel and other guests attended.

Promotion Selections

Selections to Captain and Commander were announced by the Fiscal Year 1971 Reserve Selection Board for officers in the Staff Corps. There was one officer selected in the Naval Reserve for Captain:

Dental Corps	NRRC
Messina, Richard J.	3-14

Other officers selected in the Research Reserve were as follows:

Commander, Medical Service Corps	NRRC
Grier, Charles P.	8-12
McCarthy, Thomas	5-10
Neill, Viola M. (WAVE)	12-3
Richardson, Lavon P.	8-13

Commander, Dental Corps	NRRC
Barrett, Darwin S.	12-3
Dattilo, Bruno F.	4-1
Moffitt, Richard E.	13-5

(Continued from Page 28)

Dr. Pomerantz approached the problem with the theory that slight alterations in fluid volumes within the lungs should change the electrical impedance of the lung. He then developed a technique which in experimental and clinical studies confirmed that these alterations can be accurately monitored through the measurement of thoracic electrical impedance. The method is simple, rapid and does not involve invasion of the body. It employs circular skin electrodes placed around the neck and abdomen which provide a field relatively uninfluenced by movement of the chest wall. This technique for early detection of pulmonary edema permits initiation of treatment in time to save the life of the patient.

Research Notes

Vanguard I Sets Longevity Record

Vanguard I is the first teenager in outer space. Space scientists and observers recently marked the tiny satellite's 13th birthday.

Since it was launched on March 17, 1958, Vanguard I has provided a wealth of technological information on the size and shape of the earth, and set a number of space records, as well.

Vanguard I was designed and developed by a team of scientists and engineers at the Naval Research Laboratory and was the first orbiting package to be powered by solar energy. Although it was preceded in space by two Soviet Sputniks and the US Explorer I satellite, none of these other space vehicles is still in orbit.

The 3-pound, grapefruit-size NRL satellite is the most likely candidate to become the granddaddy of all man-made space vehicles. Although its solar-powered radio equipment ceased functioning several years ago, scientists say it will remain in orbit for as long as 2,000 years.

The successes of Vanguard I set the pattern for a myriad of other space ventures in this country and abroad. It also served as a springboard for NRL's scientists to launch several series of space probes to study various aspects of radiation phenomena. NRL's latest scheduled effort, the launch of SOLRAD 10, to probe the effects of solar radiation in greater detail than ever before, is set for this year.

Vanguard I introduced much of the technology that has been applied in other U.S. satellite programs. For example, it proved that solar cells could be used for several years to power radio transmitters. Vanguard's solar cells operated for about seven years, while conventional batteries used to power a companion transmitter went dead after only 20 days.

In conjunction with the satellite's launch, NRL scientists laid out a worldwide tracking system called Minitrack. Laboratory scientists later used many of the principles embodied in this system to develop a Space Surveillance System, which can detect unannounced, radio-silent satellites passing over the U.S. These Space Surveillance stations have been turned over to another agency, but work continues to improve the system.

Improved Modeling of Ground and ASW Combat Processes

Dr. Seth Bonder of the University of Michigan under an Office of Naval Research contract is developing improved mathematical structures for the analytic modeling or simulation of combat processes involving the Navy and the Marine Corps. The principal emphasis of the work has been on characterizations of ground combat, involving mixed forcetypes, representations of the effects of mobility, and investigations of tactics for the optimal assignment of firepower against opposing force targets. The current research is focused on simulating the activities of command and control, such as search, reconnaissance and intelligence information gathering, which precede ground combat engagements and influence tactical allocation sequences.

The mathematical generalizations for ground combat appear to have applications to undersea warfare processes. Dr. Bonder has developed the concept of "intermittent visibility" as a factor in the search process. This refers to the fact that the sensor system may fail to detect a target because physical features of the environment that bar visibility, such as a mountain in the case of radar or a thermal barrier in the case of sonar, are between the target and the sensor. This factor needs to be taken into account in deciding whether or not to discontinue the search.

In addition, Dr. Bonder is also taking the approach that the allocation of search effort is affected by the response activities that follow detection. In other words, the search procedure should not be limited to detection of the target but have built into it a high degree of readiness on the part of the searcher to deal with the expected consequence, such as attack or possible evasion, when the target has been detected.

It is planned to continue to explore the applications of the research findings to related undersea warfare problems through the analyses staffs of the Navy's ASW commands as well as continue with the more obvious Marine Corps combat analyses.

Study Compares Performance of Diver Versus Manipulator

A study undertaken by the Electric Boat Division of General Dynamics under the direction of the Engineering Psychology Programs of the Office of Naval Research is comparing the performance of the diver *versus* manned operation of a submersible's manipulator in accomplishing a variety of tasks. The initial results of this research program show that where a diver and manipulator work at shallow depths under ideal conditions, the diver is on the average four times faster than the manipulator. The actual ratio, however, varies considerably depending on the nature of the task involved. In some simple tasks, such as sample collection and valve manipulation, the diver proves to be about ten times faster. On the other hand, the manipulator comes close to equalling the diver's performance in drilling and tapping holes in metal plate.

One feature of the study was that it showed that the pushbutton-controlled manipulator was generally more efficient than the joystick-operated manipulator, especially in the more complicated tasks where alignment and precise control were required. This was particularly true in drilling where the pushbutton control did 40 percent better than the joystick. It is judged that the need for slow, deliberate control under conditions of poor visibility and optical distortion were the contributing factors which resulted in the general superiority of pushbutton control over joystick control.

Results also suggested that the manipulator in certain types of tasks, such as inserting a threaded pipe into a tapped hole and connecting a quick-disconnect coupling, would come closer to matching the diver's performance if it were equipped with some means of tactile or force feed-back. During subsequent phases of the research program, performance of the diver and manipulator operator will be compared on more complex tasks which include problem-solving skills. In addition, performance will be measured using manipulator systems which incorporate greater precision of control.

New Substance Increases White Blood Cells

Dr. F. A. H. Rice of American University in a program supported by the Office of Naval Research has discovered a chemical substance called leucogenenol that has experimentally stimulated the production of white blood cells in animals without side effects. Recent experiments show that leucogenenol appears to increase the formation of germ-fighting antibodies that are produced by white cells.

Leucogenenol was originally isolated from penicillin mold by Dr. Rice. He has also found that leucogenenol occurs naturally in the liver of cows and humans, and it may well be part of the natural mechanism for controlling the normal white cell population and stimulating its increase to deal with infection. Leucogenenol is of particular interest to the Navy because it holds promise of correcting damage to white blood cells caused by exposure to nuclear radiation as well as by the drugs used to treat severe burns and injuries or to inhibit transplantation rejection.

Experiments to date have shown that when animals are injected with leucogenenol, there is an increase in the levels of a number of types of white cells. Bone marrow cells and lymphocyte cells in the spleen also increase. Mice, rabbits, dogs and monkeys have all received leucogenenol with no gross adverse effects, such as fever or toxicity. Experiments with tissue cultures have demonstrated that leucogenenol increases the metabolic rate and their replication rate of human white blood cells. There is an indication that leucogenenol apparently decreases the latent period of antibody formation thereby speeding up the production of antibodies.

Research is continuing, with the Navy looking forward to the possibility that leucogenenol therapy may be useful in the treatment of personnel exposed to radiation by not only increasing the patient's own supply of white cells but also by improving the efficiency of tissue banked bone marrow. In addition, the augmented metabolic activity indicates an increased capability of antibody synthesis which could prove useful in attacking a variety of diseases.

Satellite Navigation Equipment

The advancement of oceanographic efforts from single-ship voyages of exploration to multi-platform (ships, buoys, aircraft) detailed experiments disclosed a critical requirement for accurate position determination on a worldwide, all weather, day and night basis. The Navy Navigation Satellite System (NNSS) provided this capability and was made available to non-Navy users in the mid-1960's; however, shipboard equipments required to exploit NNSS potential were not commercially available. In mid-1966 the Office of Naval Research contracted with Mr. James Snodgrass of the Scripps Institution of Oceanography to pursue design, development and production of portable NNSS shipboard equipments for the oceanographic research vessel fleet. As a result of this effort, research vessels in 1970 have available satellite navigation systems model MX 706CA (military nomenclature AN/WRN-4) which are small (2.5 cubic feet), fully integrated (general purpose computer with an 8K memory core, touch-tone design input panel, "nixie tube" output display panel, self-test hardware and diagnostic software), easily maintainable (pluggable module spare parts system) equipment which will provide accurate (better than 0.10 nautical mile) position fix capability at about two hour intervals on a worldwide, all weather basis. Additionally, these systems are programmed to solve for the north/south component of ship's velocity (a large error source) using short-doppler sampling techniques, to provide dead-reckoning with manual or automatic entry of course and speed, and can be programmed to operate successfully should the NNSS constellation contain more than four operational satellites. The miniaturization (about one-fifth the size and weight of earlier equipments) and maintenance simplification achieved by full integration results in an ease of portability and flexible availability of these systems to meet requirements of the research vessel fleet with a minimum investment in system quantities.

While the value of this navigational system to oceanographic research is extremely great, it will also contribute to marine safety through the accurate location of navigational hazards. As an example, Tristan de Cunha, an island in the South Atlantic with numerous nearby shoal areas, is located on an existing chart (HO 3902) about one mile north and a quarter of a mile east of its true position as determined by Columbia University's R/V VEMA using an earlier model satellite navigation system.

As of the end of September, eleven of these equipments have been delivered to research vessels; an additional seventeen will be in service by the end of 1970. Approximately half of these equipments will be used by academic institutions performing oceanographic

U. S. GOVERNMENT PRINTING OFFICE : 1971 O - 424-809

research under contract to the Office of Naval Research; two equipments are being assigned to vessels of the Environmental Science Services Administration (Coast and Geodetic Survey), two to the Naval Research Laboratory, two to the Naval Electronics Systems Command and seven to the Navy Oceanographic Office.

New Theory on Cavitation Damage

The problem of cavitation, which is concerned with the generation of vapor-filled cavities in liquid flows and their subsequent collapse, arises in almost every engineering application involving the flow of water at relatively high speeds. When the cavities collapse on or near a solid surface bounding the flow such as a pipe wall, propeller blade or hydrofoil, the intensity of the force transmitted to the surface is so great that fragments of the surface are literally torn out from it. This loss of structural material, aptly referred to as cavitation damage, leads in many cases to dangerous weakening in mechanical strength and to serious impairment in hydrodynamic performance. Another highly undesirable characteristic of cavitation is the hydrodynamic noise associated with the collapse of the cavities.

Research on cavitation and cavitation damage sponsored by the Office of Naval Research is being carried out at the California Institute of Technology under the direction of Professor Milton S. Plesset. Recent results of this research have provided for the first time an accurate theoretical analysis which follows the collapse of a spherical vapor cavity near a solid boundary. The theory, based on the numerical solution of the equations governing the motion of the cavity, shows that a large deformation of the cavity shape takes place fairly early in the collapse history. Subsequently, as the cavity collapse continues, a high-speed jet of water directed toward the solid boundary is formed. Ultimately, in the analysis, the jet impacts with the solid boundary and it is conjectured that this high-speed impact generates extremely high stresses in the solid boundary which lead to cavitation damage, *i.e.*, to the loss of solid material from the surface.

The results of this theory give added insight and clarification into the mechanics of cavitation damage and will undoubtedly stimulate new research along related lines whose results will ultimately permit the engineering problems associated with cavitation and cavitation damage to be satisfactorily resolved.

NAVAL RESEARCH REVIEWS publishes highlights of research conducted by Navy laboratories and contractors and describes important naval experimental facilities. Manuscripts submitted for publication, correspondence concerning prospective articles, and changes of address, should be directed to Code 109, Office of Naval Research, Arlington, Va. 22217. Requests for subscriptions should be directed to the Superintendent of Documents, U.S. Government Printing Office, Washington, D.C., 20402. Subscription price: $1.75 per year in the U.S. and Canada; $2.25 per year, foreign; $0.20 per individual copy. The issuance of this periodical approved in accordance with Dept. of the Navy publications and printing regulations.

Editor: WILLIAM J. LESCURE

NAVSO P-510

Associate Editors:

T. B. DOWD, ONR BOSTON
L. A. WHITE, ONR CHICAGO
I. ROWE, ONR NEW YORK
E. GLOYE, ONR PASADENA
P. MILLER, ONR SAN FRANCISCO
J. DE LAUNAY, NAVAL RESEARCH LABORATORY

IN THIS ISSUE

VOL. XXIV, NO. 4

The Search for Fusion Power .... CDR G. J. MISCHKE 1

Fusion power will have a dominant role in shaping the world energy picture. Fusion power is an answer to the Navy's problem of increasing the power supply on ships and fixed installations to meet future operational requirements.

Thin Film Coatings by Sputtering .... JAMES COMAS 17

Thin film coatings by sputtering provide protective layers for passivation and radiation shielding, reflecting surfaces, and the fabrication of many electronic devices. NRL's work in this field will provide important new applications for the Navy.

On the Naval Research Reserve 29

Research Notes 30

Vanguard I, the oldest satellite in space, recently marked its 13th birthday. Vanguard was designed and developed by a team of scientists at the Naval Research Laboratory. *See page 30.*

DEPARTMENT OF THE NAVY
OFFICE OF NAVAL RESEARCH
ARLINGTON, VA. 22217

OFFICIAL BUSINESS

POSTAGE AND FEES PAID
DEPARTMENT OF THE NAVY